Combinatorial method to prepare metal nanoparticles that catalyze the growth of single-walled carbon nanotubes

Suguru Noda[a)] and Yoshiko Tsuji
Department of Chemical System Engineering, School of Engineering, The University of Tokyo, 7-3-1 Hongo, Bunkyo-ku, Tokyo 113-8656, Japan
Yoichi Murakami and Shigeo Maruyama
Department of Mechanical Engineering, School of Engineering, The University of Tokyo, 7-3-1 Hongo, Bunkyo-ku, Tokyo 113-8656, Japan

Abstract: Enhanced surface diffusion at the growth temperature of single-walled carbon nanotubes (SWNTs) can cause coarsening of metal catalysts. By balancing the nominal thickness and surface diffusion length of metals, metal nanoparticles of desirable size are expected to form spontaneously under the SWNTs growth conditions. Our combinatorial method, using a library of nominally 0.001- to 1-nm-thick sputter-deposited cobalt patterns, successfully identified in a single experimental run that cobalt nanoparticles from submonolayers can catalyze the growth of high quality SWNTs.

Since the discovery of carbon nanotubes (CNTs),[1] they are attracting much attention as promising materials for application in nanodevices due to their excellent mechanical, electrical, and chemical properties.[2,3] Many of the applications such as electron field emission sources,[4] single electron transistors,[5] field effect transistors,[6] molecular wires,[7,8] and chemical sensors[9] require controlled growth of CNTs on a variety of substrates. CNTs are grown mainly by chemical vapor deposition (CVD) on substrates with transition metal catalysts, and extensive efforts have been applied to develop the preparation methods of catalysts by both wet[7,10,11] and dry[12,13] processes. The catalyst conditions, however, depend on the processing conditions, such as the type of substrate, types of reactant gases in CVD, and CVD temperature. Such dependence makes conventional trial-and-error approaches to find preparation conditions of active catalysts time-consuming.

Aiming at efficient screening of catalyst preparation conditions, several studies have used combinatorial approaches.[14–17] Cassell et al. successfully grew multi-walled CNTs (MWNTs)[14] and single-walled CNTs (SWNTs)[15] by using catalyst libraries produced from a solution containing three components, namely, metal salts as catalyst, $SiCl_4$ or $AlCl_3$ as substrate-forming components, and triblock copolymers as "structure-directing agents". Ng et al. applied a dry process to prepare catalyst libraries of 5- to 10-nm-thick metals,[16] which yielded MWNTs. These studies confirm that combinatorial approaches are effective in the screening of catalyst preparation conditions, although the underlying mechanism that determines catalytic activity remains unclear. Kinloch et al.[17] recently studied catalyst libraries similar to those studied by Cassell et al.,[14,15] and found that "the structuring agent was not controlling the size of the catalyst particle by encapsulating the nitrate salt in micelles but rather the agent improved the wetting and hence uniformity of the catalyst precursor spot." Catalyst nanoparticles appear to have structures controlled by some spontaneous processes rather than by artificial efforts applied in those studies.[14,15,17]

Metal nanoparticles are generally believed to catalyze growth of CNTs of diameter similar to theirs.[18–20] To catalyze the growth of SWNTs, catalyst nanoparticles should have diameters as small as 0.4–3 nm. Such tiny nanoparticles often suffer from their aggregation and coarsening at the elevated temperatures required for CVD. The structural evolution of

[a)] Electronic mail: noda@chemsys.t.u-tokyo.ac.jp

islands (nanoparticles) has been extensively studied in vapor deposition systems.[21] Many elementary processes contribute to the nucleation and growth of islands, but the overall process can be briefly explained as; deposits form single islands with structures near equilibrium within their surface diffusion length and these islands distribute on substrate surfaces at a spacing corresponding to the surface diffusion length. If the amount of metals within the surface diffusion length is limited, the metals will spontaneously form tiny islands under CVD conditions. However, predicting the amount (nominal thickness) of metals to yield the nanoparticles of desirable sizes is difficult because estimating the surface diffusion lengths is almost impossible for most metal/substrate systems.

In this study, to discover spontaneously formed nanoparticles which can catalyze the growth of SWNTs, we screened the nominal thickness of metals by using a combinatorial method that we previously developed. A library of Co patterns with a wide range of nominal thickness was prepared on a Si wafer with thermal oxide by using the "*combinatorial masked deposition (CMD)*" method,[22] in which Co was sputter-deposited through holes in a mask set 2 mm above the substrate. The role of masks used in our study, however, differs; Ng et al.[16] used shadow masking to physically separate the sequentially prepared catalyst ensembles, whereas we used such masking to dilute the deposition flux at different degrees among holes of different sizes in one deposition run. In our study, each Co pattern had a radial nominal thickness profile (i.e., at different distances from the center of the sample, d_c) estimated as shown in Fig. 1 according to our previous work.[22] A wide range of nominal Co thickness (t_{Co}) between 0.001 and 1 nm could thus be examined; the t_{Co} profile within each pattern enables investigation of t_{Co} continuously, whereas the different patterns enable investigation of t_{Co} for a wide range. SWNTs were grown on the library by alcohol catalytic CVD (ACCVD).[23] Briefly, the library was placed in a hot-wall quartz-glass tubular reactor and heated to a target temperature of 1073 K under a 3 vol.% H_2/Ar flow at 40 kPa, and ACCVD was carried out by flowing ethanol vapor at 1.3 kPa for 10 min. The samples were then characterized by using field emission scanning electron microscopy (FE-SEM, Hitachi S-900 and S-4700), transmission electron microscopy (TEM, JEOL 2000EX), and micro-Raman scattering spectroscopy (Seki Technotron, STR-250).

The prepared Co patterns were so thin that they could not be discriminated by the naked eye. After ACCVD, however, these patterns blackened into either radial or ring-shaped visible patterns. The samples were then characterized (at the central position of each sample, d_c =0) by micro-Raman scattering measurements at 488 nm excitation (Fig. 2). The sharp and branched peak of G-band (at around 1590 cm^{-1}) with very small D-band (at around 1350 cm^{-1}) and the radial breathing mode (RBM, at around 150-280 cm^{-1}) at right resonant Raman shifts demonstrate the generation of high purity SWNTs as our previous dip-coat sample.[25] The very small D-band along with FE-SEM and TEM observations (shown later) shows the negligible amount of amorphous carbon and MWNTs. As t_{Co} decreased from pattern #1 to #7, the signals of SWNTs first increased and then decreased, and showed a maximum at $t_{Co} \approx$ 0.1- 0.3 nm (#2 to #4). Each pattern was analyzed in more detail with spatial resolution, i.e., various d_c. Fig. 2c shows the relative yield[25] of SWNTs for pattern #4 at different d_c. Again, with decreasing t_{Co} from 10^{-1} to 10^{-2} nm, the relative yield first increased and then decreased. These results show that submonolayer Co catalyzes the growth of SWNTs and that there is an optimum t_{Co} as a catalyst for SWNTs. For the conditions studied here, the optimum t_{Co} was around 0.1 nm.

Figure 3 shows plan-view FE-SEM images of patterns #3 (a) and #4 (b-d) after ACCVD. In the high magnification image (Fig. 3a), both spontaneously formed nanoparticles and SWNTs were clearly observed. Nanoparticles also appeared to have various sizes but many were 3-5-nm-sized. The real size of these nanoparticles might be smaller due to the spatial resolution limit of FE-SEM. SWNTs had a variety of structures from thick bundles to thin bundles or even maybe individuals. In the low magnification images (Fig. 3b-d), we can

see the effect of the nominal Co thickness on the nanoparticles and SWNTs. At d_c where t_{Co} was relatively thick (b,c), thick bundles of SWNTs overlapping with each other were observed, whereas for that with thinner t_{Co} (d), thinner bundles or maybe individual SWNTs were observed at lower surface coverage. Enlarged images (insets) show the nanoparticles. Comparison between (b) and (c) shows that more SWNTs were evident for (c) than (b), coinciding with the results shown in Fig. 2c, whereas fewer nanoparticles were observed for (c) than (b). This apparently contradictory relationship between the number density of SWNTs and that of nanoparticles can be understood by the possible size distribution in nanoparticles. The relatively large nanoparticles observed in the insets (5- 10 nm, or might be smaller due to the spatial resolution limit of FE-SEM) were probably catalytically inactive, and the smaller nanoparticles (< 5 nm, which cannot be observed in the low magnification images) catalyzed the growth of SWNTs.

Figure 4 shows high-resolution TEM (HR-TEM) images of as-grown SWNTs (at t_{Co} = 0.10 nm) transferred from the substrate to a TEM grid. They clearly show that our sample was high-quality SWNTs with negligible amounts of amorphous carbon and MWNTs. Some nanoparticles can also be observed. They would be either the Co nanoparticle catalysts or the large Co nanoparticles catalytically inactive.

Figure 5 qualitatively shows possible size distributions of Co nanoparticles spontaneously formed under the CVD conditions used here. For a thick t_{Co}, Co nanoparticles with a large mean diameter (around 5– 10 nm) will be formed (b). A small proportion of such nanoparticles will have a diameter suitable to catalyze SWNTs growth. Here, we suggest that the diameter range of SWNTs generated by the ACCVD method at this CVD temperature is fixed as about 0.7-1.8 nm. Hence, the size range of active nanoparticle size should be similar to the diameter range.[26] With decreasing t_{Co}, the size of Co nanoparticles decreases and the number of nanoparticles with a diameter similar to that of SWNTs increases (c), resulting in a higher yield of SWNTs (Fig. 3c). SWNTs with a high number density will come into contact with each other during growth, resulting in the formation of thick bundles (Fig. 3c). When t_{Co} further decreases and the mean diameter of nanoparticles becomes smaller than that of SWNTs, a smaller proportion of Co nanoparticles will be catalytically active (d), resulting in a lower yield of SWNTs (Fig. 3d). SWNTs with a low number density will not often come into contact with each other, resulting into thin bundles or individual SWNTs (Fig. 3d).

In summary, we utilized metal nanoparticles spontaneously formed under SWNTs growth conditions as SWNTs catalysts. Because the size and number density of metal nanoparticles strongly depend on the surface diffusion length of metals, and because predicting the surface diffusion length is too difficult for most metal/substrate systems, the *CMD* method[22] was applied to systematically investigate Co layers of a wide range of nominal thickness. Our combinatorial method successfully identified in a single experimental run that Co nanoparticles derived from nominal submonolayers are effective in catalyzing the growth of high quality SWNTs during ACCVD. This method can be applied to a wide variety of metal/substrate systems and CVD conditions to discover SWNTs catalysts. Furthermore, the catalyst preparation conditions, i.e., nominal thicknesses of metals, derived by this method are expected to be applicable to other catalyst preparation methods, including wet processes, because the spontaneous process during CVD will govern the structure of nanoparticles. Our combinatorial method is very simple, just setting a mask with holes above a substrate during sputter-deposition of catalyst metals, and therefore it will be a powerful tool to discover heterogeneous SWNTs catalysts.

Acknowledgements: The authors thank Mr. T. Nishii of J-Power Co., Ltd. for his helps in the FE-SEM observations. They also thank Mr. H. Tsunakawa for his assistance in TEM observations. This work was financially supported in part by the “Establishment of

Networked Knowledge System with Structured Knowledge for Future Scientific Frontier Project" of JSPS, and by the "Structuring Knowledge on Materials Technology Project" of NEDO.

References:

[1]S. Iijima, Nature **354**, 56 (1991).
[2]R. Saito, G. Dresselhaus, and M. S. Dresselhaus, *Physical Properties of Carbon Nanotubes* (Imperial College Press, London, 1998).
[3]M. S. Dresselhaus, G. Dresselhaus, and P. Avouris, *Carbon Nanotubes* (Springer, Berlin, 2001).
[4]W. A. Deheer, A. Chatelain, and D. Ugarte, Science **270**, 5239 (1995).
[5]M. Bockrath, D. H. Cobden, P. L. McEuen, N. G. Chopra, A. Zettl, A. Thess, and R. E. Smalley, Science **275**, 1922 (1997).
[6]S. J. Tans, A. R. M. Verschueren, and C. Dekker, Nature **393**, 49 (1998).
[7]A. M. Cassell, N. R. Franklin, T. W. Tombler, E. M. Chan, J. Han, and H. Dai, J. Am. Chem. Soc. **121**, 7975 (1999).
[8]Y. Homma, Y. Kobayashi, T. Ogino, and T. Yamashita, Appl. Phys. Lett. **81**, 2261 (2002).
[9]J. Kong, N. R. Franklin, C. Zhou, M. G. Chapline, S. Peng, K. Cho, and H. Dai, Science **287**, 622 (2000).
[10]J. Kong, H. T. Soh, A. M. Cassell, C. F. Quate, and H. Dai, Nature **395**, 878 (1998).
[11]Y. Murakami, S. Chiashi, Y. Miyauchi, M. Hu, M. Ogura, T. Okubo, and S. Maruyama, Chem. Phys. Lett. **385**, 298 (2004).
[12]R. Y. Zhang, L. Amlani, J. Baker, J. Tresek, and R. K. Tsui, Nano Lett. **3**, 731 (2003).
[13]Y. J. Jung, Y. Homma, T. Ogino, Y. Kobayashi, D. Takagi, B. Wei, R. Vajtai, and P. M. Ajayan, J. Phys. Chem. B **107**, 6859 (2003).
[14]A. M. Cassell, S. Verma, L. Delzeit, M. Meyyappan, and J. Han, Langmuir **17**, 260 (2001).
[15]B. Chen, G. Parker II, J. Han, M. Meyyappan, and A. M. Cassell, Chem. Mater. **14**, 1891 (2002).
[16]H. T. Ng, B. Chen, J. E. Koehne, A. M. Cassell, J. Li, J. Han, and M. Meyyappan, J. Phys. Chem. B **107**, 8484 (2003).
[17]I. A. Kinloch, M. S. P. Shaffer, Y. M. Lam, and A. H. Windle, Carbon **42**, 101 (2004).
[18]H. Dai, A. G. Rinzler, P. Nikolaev, A. Thess, D. T. Colbert, and R. E. Smalley, Chem. Phys. Lett. **260**, 471 (1996).
[19]S. Helveg, C. López-Cartes, J. Sehested, P. L. Hansen, B. S. Clausen, J. R. Rostrup-Nielsen, F. Abild-Pedersen, and J. K. Nørskov, Nature **427**, 426 (2004).
[20]T. Ichihashi, J. Fujita, M. Ishida, and Y. Ochiai, Phys. Rev. Lett. **92**, 215702 (2004).
[21]C. Ratsch and J. A. Venables, J. Vac. Sci. Technol. A **21**, S96 (2003).
[22]S. Noda, Y. Kajikawa, and H. Komiyama, Appl. Surf. Sci. **225**, 372 (2004).
[23]S. Maruyama, R. Kojima, Y. Miyauchi, S. Chiashi, and M. Kohno, Chem. Phys. Lett. **360**, 229 (2002).
[24]R. Saito, G. Dresselhaus, and M. S. Dresselhaus, Phys. Rev. B **61**, 2981 (2000).
[25]Y. Murakami, Y. Miyauchi, S. Chiashi, and S. Maruyama, Chem. Phys. Lett. **377**, 49 (2003).
[26]Y. Shibuta and S. Maruyama, Chem. Phys. Lett. **382**, 381 (2003).

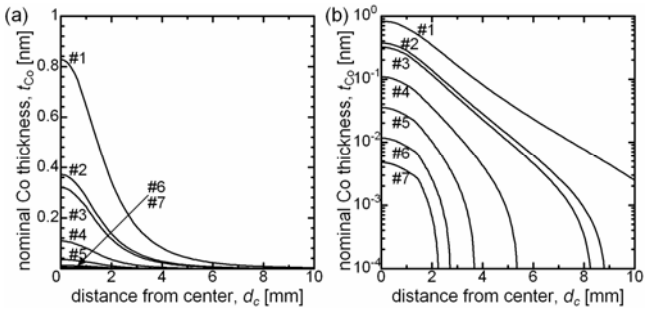

FIG. 1. Radial profiles (d_c) of nominal Co thickness t_{Co} in (a) linear and (b) logarithmic scales for seven patterns formed by *CMD* on an a-SiO_2/Si wafer. t_{Co} was estimated according to a previously described method.[22]

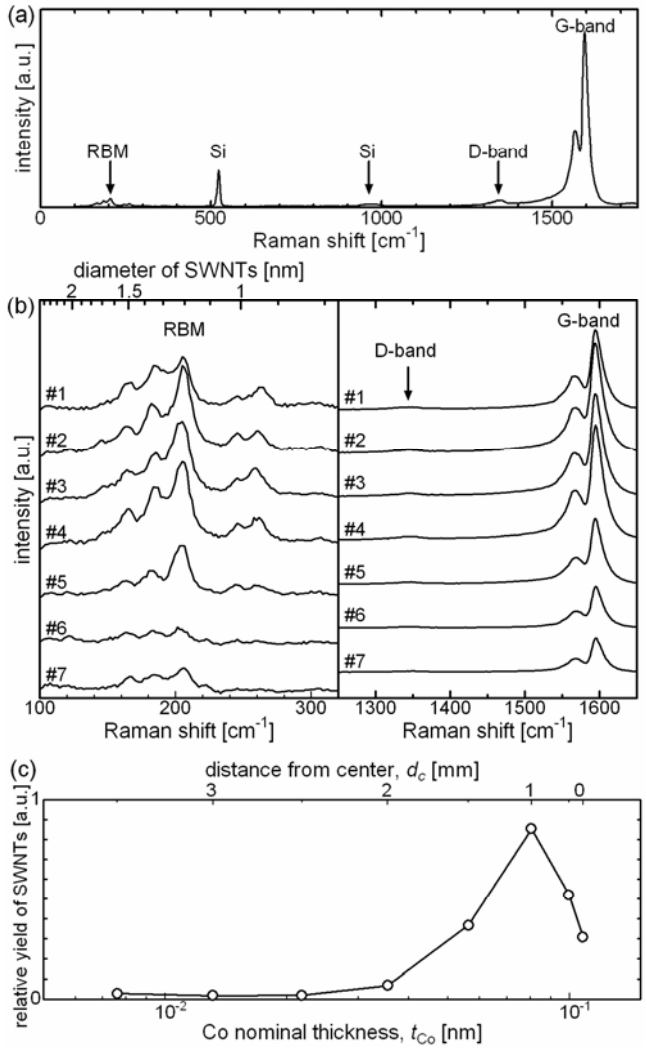

FIG. 2. Raman spectra measured for Co patterns after ACCVD by 488 nm excitation. (a) A typical Raman spectrum for our sample. (b) Raman spectra measured for each Co pattern at center location of each sample. Diameter of SWNTs was estimated by using the relationship, *diameter [nm] = 248 / Raman shift [cm^{-1}]*.[24] (c) Relative yields of SWNTs calculated from the peak ratio of G-band (1590 cm^{-1}) to Si (520 cm^{-1}) for Co pattern #4 at different d_c.

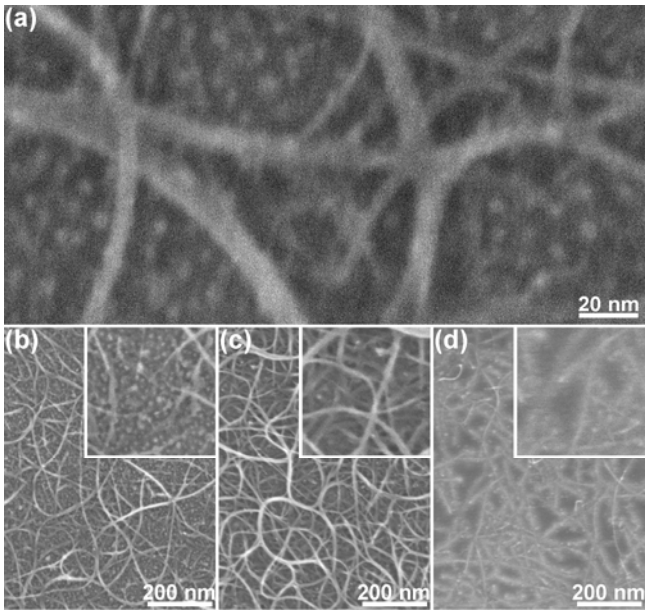

FIG. 3. Plan-view FE-SEM images of patterns #3 (a) and #4 (b-d) after ACCVD at different distances from the sample center (d_c) and estimated nominal Co thickness (t_{Co}). (a) High magnification image of d_c = 0.7 mm and t_{Co} = 0.27 nm, and low magnification images of (b) d_c = 0 mm and t_{Co} = 0.11 nm, (c) d_c = 1 mm and t_{Co} = 0.081 nm, and (d) d_c = 2 mm and t_{Co} = 0.036 nm. Insets in (b)-(d) show images at twice the magnification.

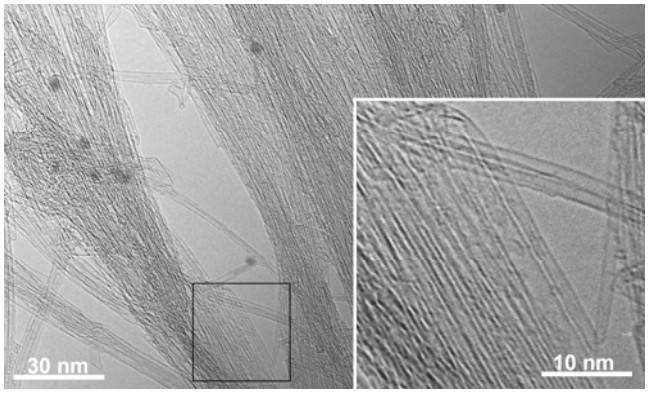

FIG. 4. HR-TEM images of as-grown SWNTs for t_{Co} = 0.10 nm. Inset shows the higher magnification image of the location indicated with a solid square in the lower magnification image.

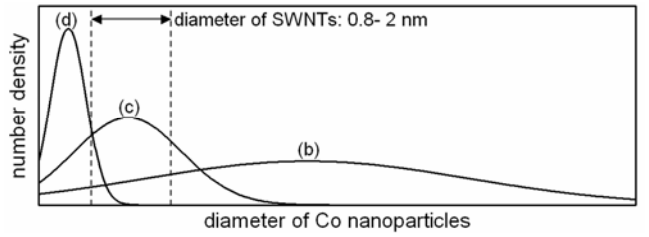

FIG. 5. Possible size distributions of Co nanoparticles to qualitatively explain the yield of SWNTs at different t_{Co}. Symbols (b)–(d) correspond to those in Fig. 3.